Journal of Applied Mechanics and Technical Physics, Vol. 47, No. 2, pp. 266–273, 2006

MATHEMATICAL MODELING FOR ONE NEW METHOD OF BREAKING ICE COVER

V. I. Odinokov and A. M. Sergeeva

UDC 539.3

The spatial problem of determining the stress–strain state of an ice plate of finite thickness broken by a patented method is solved using the theory of small elastoplastic strains and a proven numerical method.

Key words: *ice cover breakup, stresses, strains.*

Introduction. The extension of the navigation season, especially in northern seas, is an important problem. This is demonstrated by numerous patents concerned with developing methods for breaking ice cover [1]. In the present paper, a mathematical model for a new technological process of ice cover breakup is constructed. The process is patented [2] and allows breakup of ice of up to three meters thick. The idea of the method is that an evacuated space of necessary dimensions is produced under ice, and the latter breaks up under the action of its own weight and ambient atmospheric pressure. To implement this method, a container having two cheek plates moving in a horizontal direction perpendicular to the waterway (Fig. 1) is placed under ice. The two side walls and the bottom prevent water from filling the container when the cheek plates are moved apart. From the outer edges, the container is fully open (there is only a drive for moving the cheek plates), and the removal of water by the cheek plates is not hindered. The rate of motion of the cheek plates v and the container depth h should be such that when the cheek plates are moved apart a distance at which ice breakup begins, the water fills the container through the available gaps by not more than 2/3 of its volume.

A calculation of the filling of the container with water was performed in [3]. The rate of separation displacement of the cheek plates is given by the analytical formula

$$v = 3M/(2bh), \tag{1}$$

where

$$M = \delta\sqrt{\frac{2\sigma_0 q}{\gamma}}\,(b_1 + l) + \frac{4}{3}\,\delta\sqrt{2q}\left[\left(\frac{\sigma_0}{\gamma} + h\right)^{3/2} - \left(\frac{\sigma_0}{\gamma}\right)^{3/2}\right] + \delta b\sqrt{2q\left(\frac{\sigma_0}{\gamma} + h\right)}.$$

Here l is the displacement of the cheek plates from the vertical plane of symmetry, δ is the gap between the movable cheek plates and the motionless parts of the container, and, hence, the ice plate, q is the gravity acceleration, γ is the relative water density, σ_0 is the atmospheric pressure, and $b_1 = 2b$ is the total width of the container.

Formulation and Solution of the Problem. The spatial problem of the strain of ice cover under atmospheric pressure and the weight of ice is solved. Since the problem is symmetric, we consider one-fourths of the strain area (Fig. 2a). Formalizing the deformation model, we assume that ice I rests on the container case II and the elastic foundation (water) outside the container. Inside the container, ice is deflected under the action of its own weight and ambient atmospheric pressure. The medium being deformed is considered elastic and isotropic, and the elastic displacements small. Inertia forces are ignored because of the smallness of the rate of separation displacement of the cheek plates. Using the equations of the theory of elasticity for small strains, we write the following system of differential equations in Cartesian coordinates:

Institute of Machine Science and Metallurgy, Far East Division, Russian Academy of Sciences, Komsomol'sk-on-Amur 681005; mail@imim.ru. Translated from Prikladnaya Mekhanika i Tekhnicheskaya Fizika, Vol. 47, No. 2, pp. 139–146, March–April, 2006. Original article submitted February 11, 2005; revision submitted April 7, 2005.

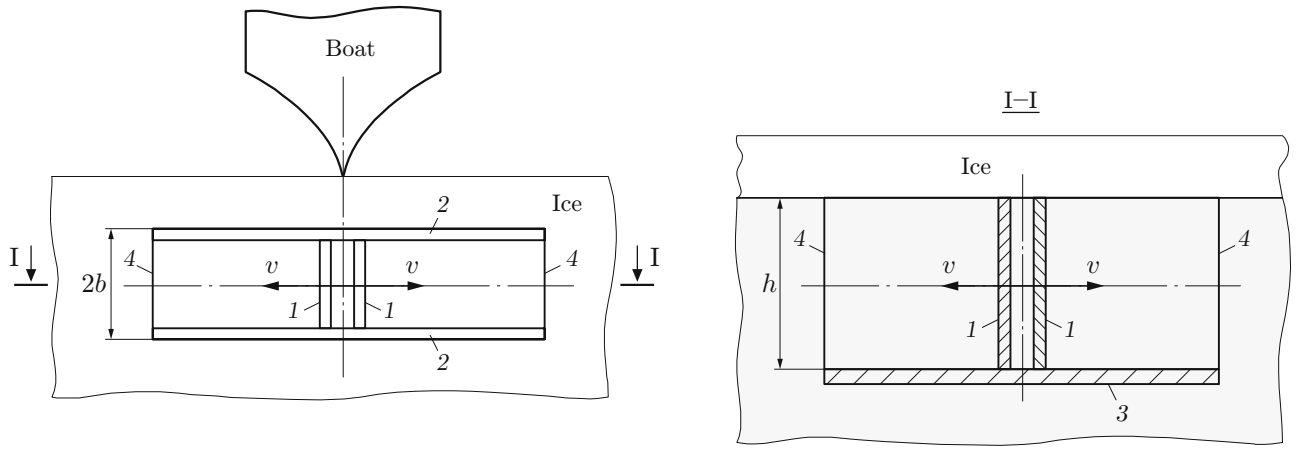

Fig. 1. Diagram illustrating the formation of an evacuated space under ice: movable cheek plates (1), side walls (2), bottom (3), and outer edges of the container (4).

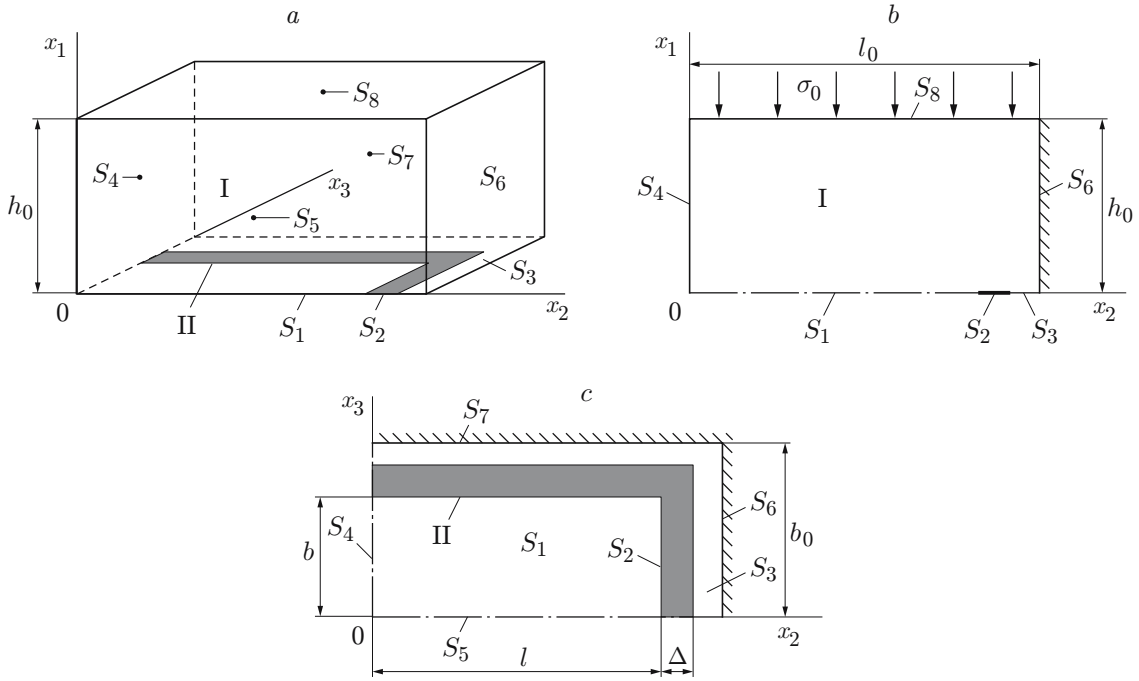

Fig. 2. Diagram of strain calculations for the ice plate: spatial diagram (a) and diagrams in the planes x_1x_2 (b) and x_2x_3 (c).

$$\sigma_{ij,j} + F_i = 0, \quad i,j = 1,2,3, \qquad F_2 = F_3 = 0; \tag{2}$$

$$\sigma_{ij} - \sigma\delta_{ij} = 2G\varepsilon^*_{ij}, \quad i,j = 1,2,3, \qquad \varepsilon^*_{ij} = \varepsilon_{ij} - (1/3)\varepsilon\delta_{ij}, \qquad \varepsilon = \varepsilon_{ii},$$

$$\sigma = \frac{1}{3}\sigma_{ii}, \qquad \varepsilon_{ij} = \frac{u_{i,j} + u_{j,i}}{2}, \qquad \delta_{ij} = \begin{cases} 1, & i = j \\ 0, & i \neq j \end{cases} \tag{3}$$

$$\varepsilon_{ii} = 3k\sigma. \tag{4}$$

The thermal heat conductivity equation for the stationary case is written as

$$\frac{\partial}{\partial x_i}\Big(\lambda \frac{\partial\theta}{\partial x_i}\Big) = 0. \tag{5}$$

In (2)–(5), $G = G(\theta)$ is the shear modulus, θ is the temperature, $k = k(\theta)$ is the bulk compression coefficient, σ_{ij} are the stress tensor components, ε_{ij} are the strain tensor components, F_i are projections of the specific bulk force onto the x_i axes, u_i are projections of displacements onto the coordinate axes x_i ($i = 1, 2, 3$), and λ is the thermal conductivity. Equations (2)–(5) are written with allowance for summation over repeated indices.

Ice cover can be treated as a plate of finite thickness in which

$$\frac{\partial\theta}{\partial x_2} = \frac{\partial\theta}{\partial x_3} = 0.$$

Then, Eq. (5) becomes

$$\frac{\partial}{\partial x_1}\Big(\lambda\,\frac{\partial\theta}{\partial x_1}\Big) = 0 \tag{6}$$

with the boundary conditions $\theta|_{x_1=0} = 0$ and $\theta|_{x_1=h} = \theta_1$. The coefficient $\lambda(\theta)$ varies with temperature according to the linear law [8]

$$\lambda = \lambda_0(1 + a\theta). \tag{7}$$

Integrating Eq. (6) and setting $\theta_0 = 0$, we obtain

$$\theta = -\frac{1}{a} + \sqrt{\Big(\frac{1}{a}\Big)^2 + \frac{x_1}{h}\Big(\frac{2\theta_1}{a} + \theta_1^2\Big)}\,. \tag{8}$$

According to the data of [8], $a = -0.0159$ and $\lambda_0 = 2.22$ W/(m·K).

The boundary conditions of the problem are given by

$$\begin{gathered}
\sigma_{11}|_{S_8} = -\sigma_0, \qquad (\sigma_{12} = \sigma_{13})|_{S_8} = 0, \qquad (\sigma_{11} = \sigma_{12} = \sigma_{13})|_{S_1} = 0,\\
(\sigma_{12} = \sigma_{13})|_{S_3} = 0, \qquad \sigma_{21}|_{S_4} = 0, \qquad \sigma_{23}|_{S_i} = 0 \quad (i = 4, 6);\\
(\sigma_{12} = \sigma_{13})|_{S_2} = 0, \qquad \sigma_{31}|_{S_5} = 0, \qquad \sigma_{32}|_{S_i} = 0 \quad (i = 5, 7);\\
\sigma_{11}|_{S_3} = -q_1, \qquad \sigma_{11}|_{S_2} = \sigma_*, \qquad u_2|_{S_i} = 0 \quad (i = 4, 6), \qquad u_3|_{S_i} = 0 \quad (i = 5, 7),
\end{gathered} \tag{9}$$

where $q_1 = \sigma_0 + \gamma h_*$ (h_* is the depth of dip of ice).

We note that the container filled with water has positive buoyancy. The separation displacement of the cheek plates of the container gives rise to a force which is directed from below the container sides to the ice. This force arises from the action of atmospheric pressure and the displaced water due to the cavity formed in the container. Then, the buoyant force is $P = blh_1\gamma$, where h_1 is the height of the cavity formed in the container ($h_1 < h$ because water flows inward during the separation displacement of the cheek plates), γ is the relative density of water; and σ_0 is atmospheric pressure.

Hence, the stresses on the container sides S_2 (see Fig. 2) are calculated by the formula

$$\sigma_* = -P/[(l + \Delta)\Delta + b\Delta] = \sigma_{11}|_{S_2}. \tag{10}$$

That is, the separation displacement of the cheek plates results in the formation of a free space under the ice plate, and ice, being deformed, begins to immerse, together with the container, in water under the action of its own weight and ambient atmospheric pressure. On the outer faces S_6 and S_7 (Fig. 2), we assume that the ice is fastened and cannot move into water. This simulates the relationship between the examined ice pillow and the external undeformable foundation. This relationship is given by the equations [7]

$$\sigma_{21}|_{S_6} = -\psi_6\tau_S v_{\text{slid}}/|v|; \qquad \sigma_{31}|_{S_7} = -\psi_7\tau_S v_{\text{slid}}/|v|. \tag{11}$$

Here $\psi_6 = \psi_7 = 1000$ and v_{slid} is the rate of sliding of the ice pillow relative to the foundation ($v_{\text{slid}} = v_1|_{S_3} - v_1^*$, where v_1^* is the rate of motion of the foundation). In our case, $v_1^* = 0$, $|v|$ is the normalizing rate, and τ_S is the conditional yield limit of ice. Calculations show that for the adopted values of ψ_i ($i = 6, 7$) the displacement u_1 near S_6 and S_7 is 0.0007 mm. In this case, the tangential stresses on the surfaces S_6 and S_7 do not exceed 0.02 MPa.

To solve the system of differential equations (2)–(4) subject to constraint (8) and boundary conditions (9)–(11), we use the numerical method of [5]. According to this method, the strain region is broken into orthogonal elements of finite sizes; for each element, system (2)–(4) is written in difference form and is solved using the algorithm developed with allowance for the mixed boundary conditions (9). As a result, we have the stress field σ_{ij} and the displacement field u_i on the faces of each element.

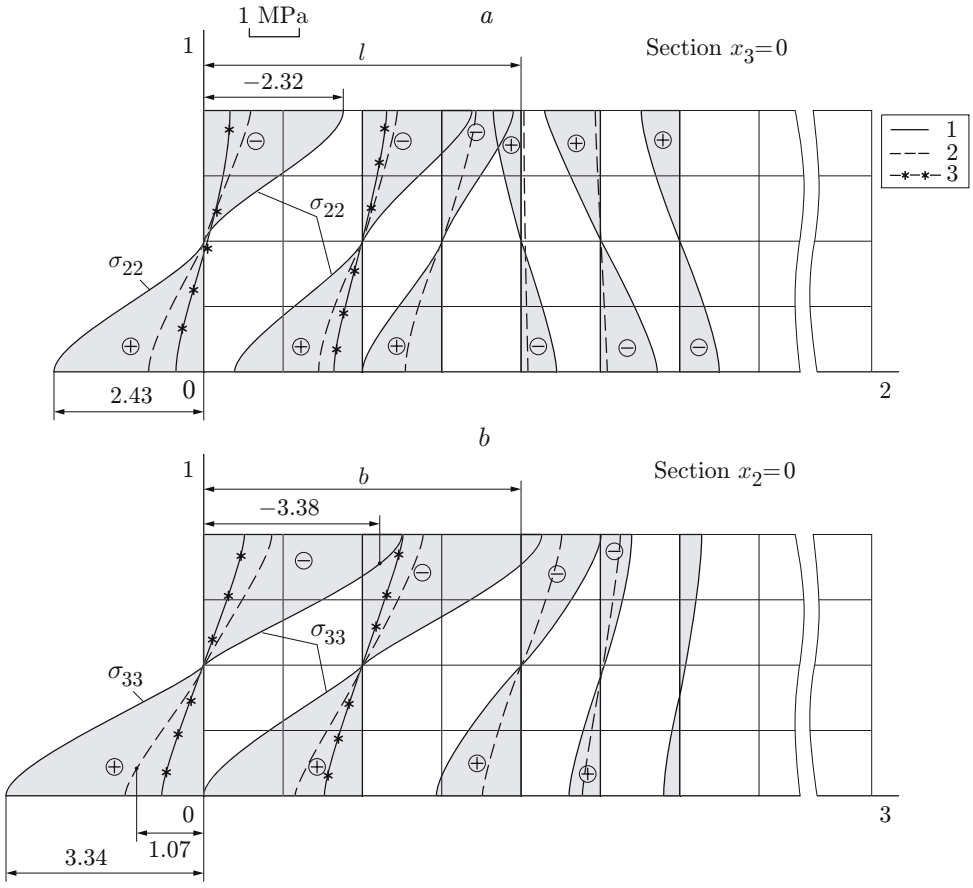

Fig. 3. Diagrams of the stresses σ_{22} (a) and σ_{33} (b) for various ice thickness: $h_0 = 1$ (1), 2 (2), and 3 m (3); $h_1 = 2$ m, $l = 10$ m, $b = 3$ m, $l_0 = 20$ m, $b_0 = 13$ m, and $\delta = 1$.

In implementing the indicated numerical method, we used the numerical scheme developed in [6] to solve spatial problems, according to which the basic system of difference equations is convolved into an equivalent system which has an order of magnitude smaller number of unknowns than the basic system. The algorithm developed in [7] is used to calculate the matrix of the new equivalent system, which is solved using a standard program.

The modeling was performed using the properties of fresh-water ice. It should be noted that fresh-water ice is stronger than sea ice.

According to [4], $E = (87.6 - 0.21\theta - 0.0017\theta^2) \cdot 10^2$ MPa, the Poisson's ratio $\nu = 0.5 + 0.003\theta$ ($\theta > -40°$C), the bulk compression coefficient $k = (1 - 2\nu)/E$, and the shear modulus $G = E/(2(1 + \nu))$.

In formula (8), we set $\theta_1 = -30°$C.

The algorithm of solution of the problem is as follows.

1. Initial conditions are specified.

2. The strain regions being studied is broken into elements of orthogonal shape. The matrix of the arc lengths of the elements is calculated.

3. The matrix of the boundary conditions is specified according to (9).

4. The temperature field for each element is calculated by formula (8).

5. The values of $(G)_n$ and $(k)_n$ for each element (n is the element number) are calculated using the formulas given above.

6. The matrix of the coefficients and free terms of the new equivalent system is calculated in accordance with the sequence of calculations indicated above.

7. The system of the linear equations is solved using the standard program.

8. The values of σ_{ij} and u_i are calculated for each element (for its faces IJ).

9. The completion of the calculation.

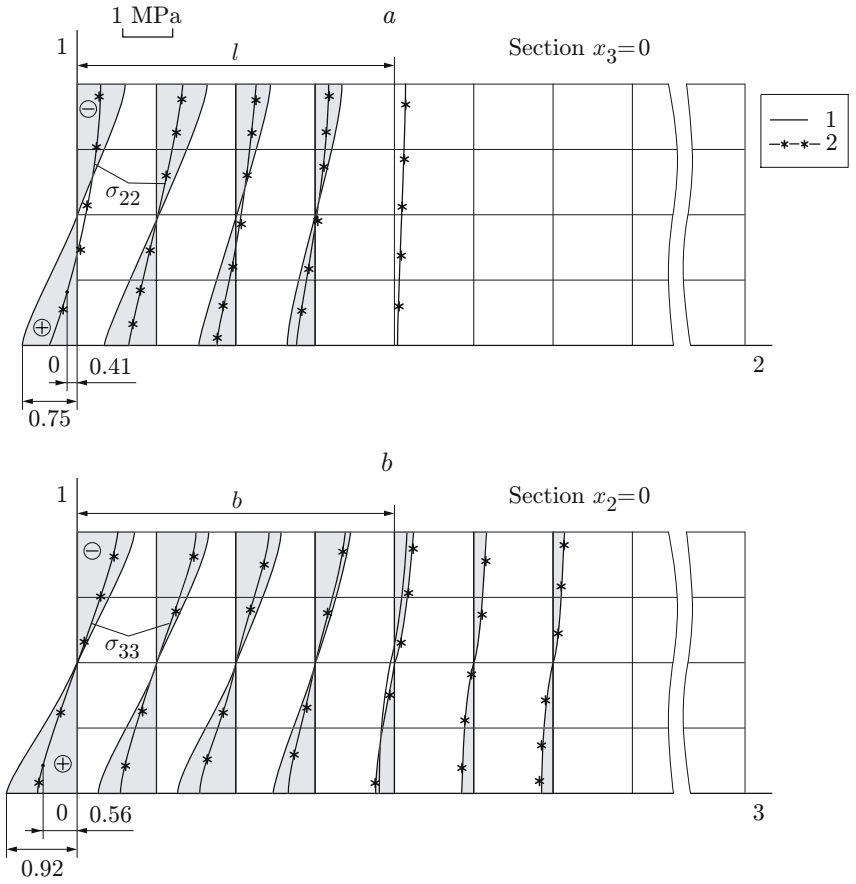

Fig. 4. Diagrams of the stresses σ_{22} (a) and σ_{33} (b) for $b = 5$ (1) and 3 m (2); $h_1 = 2$ m, $l = 10$ m, $l_0 = 20$ m, $h_0 = 3$ m, and $\delta = 1$.

Results. Figure 3 gives diagrams of the stresses σ_{22} (a) and σ_{33} (b) for various ice thicknesses $h_0 = 1$, 2, and 3 m. As one might expect, the tensile stresses decrease with increase in the ice thickness. The largest values of the tensile stresses are reached at the bottom of the ice in the center of the plane $x_2 = 0$ (see Fig. 3b). It is interesting to note that the diagram of the stress σ_{22}, passing the container side in the plane $x_3 = 0$, changes qualitatively in nature (see Fig. 3a), whereas the diagram of the stress σ_{33} in the plane $x_2 = 0$ (Fig. 3b), passing through the side, remains qualitatively the same, decaying monotonically to the edge $x_3 = b_0$. The calculation results show that ice breakup certainly occurs for $h_0 = 1$ and 2 m and most likely for $h_0 = 3$ m. The strength limit of the ice for the bending of a cut standard sample is 2–3 MPa. Usually, the experimental strength for ice rafts of large sizes is several orders of magnitude lower than laboratory data and is $\sigma_{\text{strength}} = 0.04$–$0.09$ MPa [8], i.e., the scale factor is of great significance in these experiments. Diagrams of the tangential stresses σ_{ij} $(j \neq i)$ are not given in the paper since they are smaller than the normal stresses by approximately an order of magnitude and are not determining for ice breakup in this case.

Figure 4 shows diagrams of the stresses σ_{22} and σ_{33} for $h_0 = 3$ m and $b = 3$ and 5 m. The values of the tensile stresses increase almost proportionally to the increase in b.

Figure 5 shows how the diagrams of the stresses σ_{22} and σ_{33} vary as the container is filled with water, i.e., as the value of h_1 varies. The results show that as the container is filled with water, the pressure of container side on the ice decreases and the container is more strongly drowned by the mass of ice and, consequently, the ice is more intensively deformed, as is suggested by an increase in the stresses σ_{22} (a) and σ_{33} (b).

As follows from Fig. 5, the stresses σ_{22} and σ_{33} depend greatly on the degree of filling of the container with water, i.e., on the pressure exerted by the container sides on the ice. The container is filled with water as the cheek plates are moving apart (see Fig. 1).

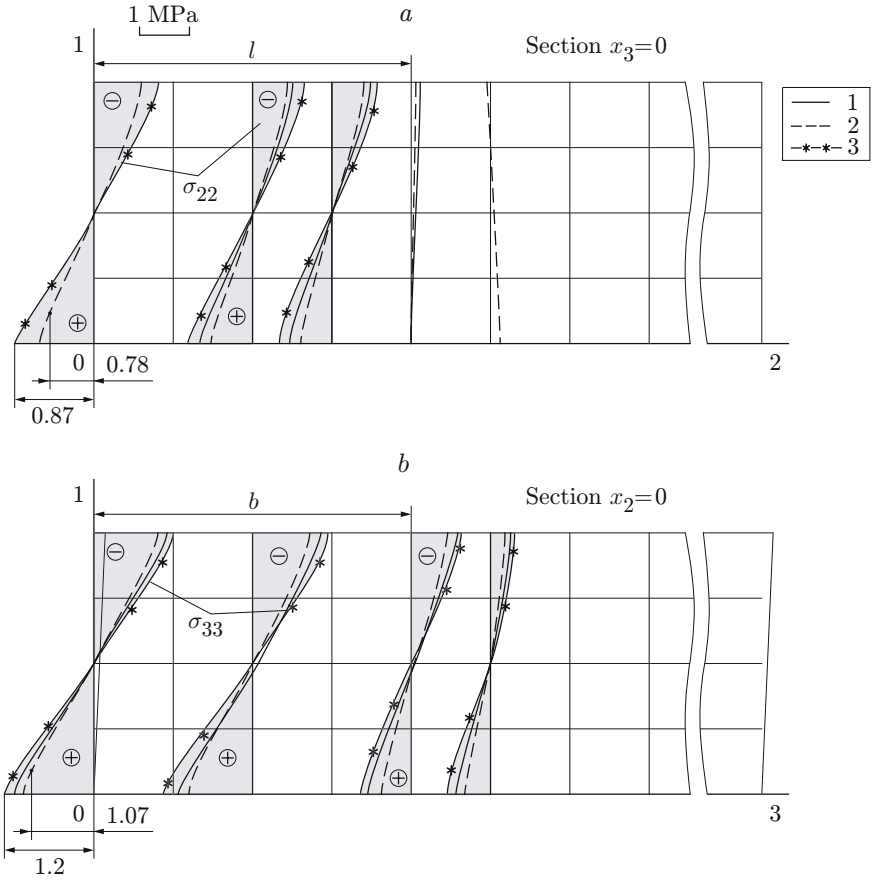

Fig. 5. Diagrams of the stresses σ_{22} (a) and σ_{33} (b) for $h_1 = 1$ (1), 2 (2), and 0.5 m (3); $b = 3$ m, $l = 10$ m, $l_0 = 20$ m, $b_0 = 13$ m, $\delta = 1$, and $h_0 = 2$ m.

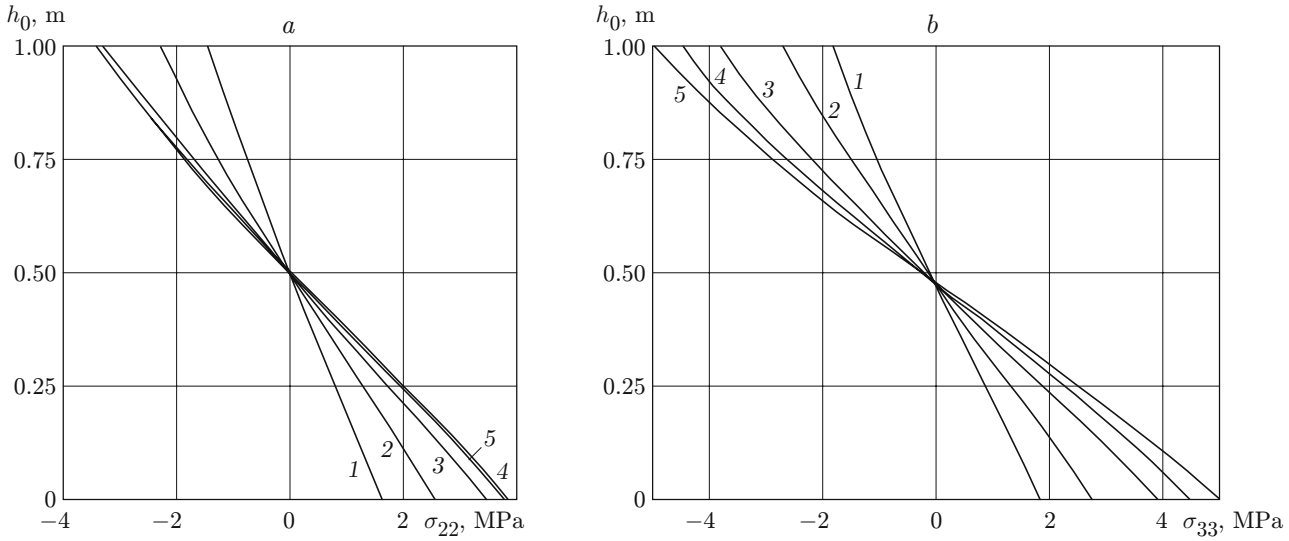

Fig. 6. Variation (by height h_0) in the stresses σ_{22} (a) and σ_{33} (b) versus the separation displacement of the cheek plates: $l = 1$ m (1), 3 (2), 6 (3), 8 (4), and 10 m (5); $l_0 = 20$ m, $b_0 = 13$ m, $b = 3$ m, $h = 3$ m, $\delta = 10$ mm, $\sigma_0 = 1$ kg/cm^2, $\gamma = 10$ kg/cm^3, $q = 10$ m/sec^2, and $v = 20$ m/min.

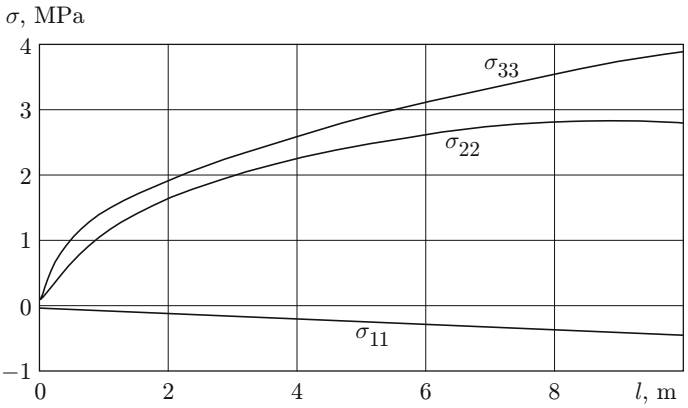

Fig. 7. Variation in the stresses σ_{11}, σ_{22}, and σ_{33} versus the separation displacement of the cheek plates for $x_3 = x_1 = 0$ (from the data of Fig. 6).

According to the formula of [3], the volume of the water filling the examined part of the container equals $V = M\tau/2 = Ml/(2v)$ (v is the rate of displacement of the cheek plates), the volume of the current part of the container is $\bar{V}_k = lbh$, and the volume of the container not filled with water is $\bar{V}_{k_1} = lbh_1$, where h_1 is the height of the space free from water (the distance from the inner surface of ice to the water surface in the container).

Thus, we write the equation $lbh_1 + Ml/v = lbh$, whence

$$h_1 = h - M/(2bv). \tag{12}$$

Let us set $b = 6$ m, $h = 3$ m, $\delta = 10$ mm, $\sigma_0 = 1$ kg/cm^2, $\gamma = 1$ kg/cm^3, $q = 10$ km/sec^2, and $v = 20$ m/min. The quantity h_1, which determines the stress on the surface S_2, is defined by formula (12).

Some results of the numerical solution are presented in Figs. 6 and 7.

The stresses σ_{22} reach the largest value on the symmetry axis $x_2 = 0$, $x_3 = 0$. Curves of $\sigma_{22}(h_0)$ are presented in Fig. 6a. In the process of separation of the cheek plates, the tensile stresses σ_{22} for $x_1 = 0$ increase to a certain value. Curves 4 and 5 almost coincide; even for $l = 8$ m, the stresses $\sigma_{22}|_{x_1=0}$ are somewhat higher than those for $l = 10$ m. Figure 6b shows the curves $\sigma_{33}(h_0)$ for $x_2 = 0$ and $x_3 = 0$. It is evident from the figure that the stress σ_{33} for $x_1 = 0$ increases as the cheek plates are separated and it is higher than the stress σ_{22} for the same values of l. Figure 7 shows the stresses σ_{22} and σ_{33} for $x_3 = x_1 = 0$ versus the separation displacement of the cheek plates. In addition, the figure shows the variation in the stress σ_{11} at the container edges during the separation of the cheeks. Although the container is increasingly filled with water, the pressure on the container edges grows. This suggests that although the container is filled with water, the volume of the cavity free from water increases more rapidly at the specified rate v.

REFERENCES

1. V. V. Bogorodskii, V. P. Gavrilo, and O. A. Nedoshivin, *Ice Breakup. Methods and Means* [in Russian], Gidrometeoizdat, Moscow (1983).
2. V. I. Odinokov and V. M. Kozin, "Method of breaking ice cover," Russian Federation Patent 2220878, Bull. No. 1, Publ. 01.10.04.
3. A. M. Polyarus and D. Yu. Romanov, "One method of breaking ice cover," in: *Problems of the Mechanics of Continuous Media and Related Issues of Mechanical Engineering*, Proc. Second Conf. (Vladivostok, Russia, August 31–September 6 2003), Inst. of Machine Science and Metallurgy, Far East Division, Russian Academy of Sciences, Komsomol'sk-on-Amur (2003), pp. 23–28.

4. V. P. Berdyannikov, "Elastic modulus of ice," *Tr. GPI*, No. 7(61), 13–23 (1948).
5. V. I. Odinokov, *Numerical Investigation of the Deformation of Materials by a Coordinate-Free Method* [in Russian], Dal'nauka, Vladivostok (1995).
6. V. I. Merkulov, V. I. Odinokov, and N. S. Lovizin, "One approach to the numerical solution of problems of elastoplastic deformation of spatial bodies," in: *Kuzn. Shtamp. Proizv. Obr. Met. Davl.*, No. 6, 12–19 (2001).
7. E. I. Makeranets and V. I. Odinokov, "Calculation of plastic flow around hollow oval cylinders of infinite length," *Izv. Akad. Nauk SSSR, Mekh. Tverd. Tela*, **2**, 103–110 (1976).
8. V. V. Bogorodskii and V. P. Gavrilo, *Physical Properties. Modern Methods of Glaciology* [in Russian], Gidrometeoizdat, Leningrad (1980).